

Plant species identification from leaf images using shape features

Charlie Hewitt
Computer Laboratory
University of Cambridge, UK
`cth40@cam.ac.uk`

Abstract

This paper presents a novel feature set for shape only leaf identification. This includes basic shape features and signal features extracted from local area integral invariants, similar to curvature maps, at multiple scales. The methodology is evaluated on a number of publicly available leaf datasets with comparable results to existing methods which make use of colour and texture features in addition to shape. Over 90% accuracy is achieved on all but one dataset, with top-four accuracy for these datasets over 98%. Rotation and scale invariance of the feature extraction process are demonstrated, along with an evaluation of the generalisability of the approach for generic shape matching.

1. Introduction

1.1. Motivation

Shape matching and classification is a long standing problem in computer vision. Plant leaf identification is a particularly interesting subset of this problem as the intra-class variation of leaf shapes is typically quite large, while interclass variation may be very small.

Many existing leaf identification techniques rely on a fusion of feature types, including shape, colour and texture. Colour features often prove quite effective in increasing accuracy on leaf datasets which typically include leaves collected only during summer. For real-world leaf classification, where colours of leaves from the same tree will vary drastically across the year and under different lighting conditions, these colour features are rendered almost completely obsolete. Texture and vein features rely on very high quality images, often aided by backlighting. Obtaining these features from lower quality field images is unrealistic.

I therefore intend to focus on purely shape-based leaf identification as shape features rely only on being able to achieve a good segmentation of the leaf from the image background. This task of segmentation is much more realistic for field images and is largely unaffected by changes

in leaf colour and lighting conditions.

For this type of image classification task, one might be tempted turn to deep learning approaches, such as LeafNet [3] which features a large CNN trained on the Leafsnap dataset achieving high classification accuracy (86.3%). There are two key issues with this approach; firstly, there is no control over the features which the CNN learns and as such non-relevant factors such as lighting conditions and background objects (e.g. scale rulers in lab images) might be considered when they are clearly not relevant to the actual problem of leaf identification. Secondly, the LeafNet CNN took many days to train and would result in extremely large storage requirements for deployment. This makes it infeasible for any practical application, where new data or leaf classes might need to be incorporated or deployment (particularly to mobile devices) is a consideration.

In light of these factors, classical machine learning is instead chosen as the primary direction for this research, with classifiers that are typically lightweight, quickly updatable and easily deployable. Local area integral invariants (LAIIs) are used to represent leaf shapes in a compact and more directly useful format for feature extraction. Similar to curvature maps, LAIIs have a number of desirable attributes for shape representation; they are translation, rotation and scale invariant.

1.2. Paper Structure

The remainder of the introduction section presents related works and a summary of publicly available leaf image datasets. Section 2 gives a description of the implementation of the system, including image preprocessing, leaf segmentation, integral invariant extraction, the selected feature set and classification procedure.

Classification results for the leaf image datasets and comments are given in Section 3, along with an evaluation of the invariance of the method to rotation and scale, and the generalisability of the approach. Section 4 provides suggestions for future work and a concise summary of the paper.

Source code for this project is available on GitHub [9].

1.3. Related Work

Shape matching is one of the most common problems in computer vision and a huge number of methods have been proposed to tackle this task with varying success. Most common methods focus on extracting some form of shape descriptors which capture the key elements of the shape irrespective of its transformation within the scene, such as shape descriptors [4], chamfers [24] and complex networks [1]. These methods are often very good at capturing large shape features and therefore good at identifying common objects which typically vary significantly in shape, but are less effective at capturing small variations such as serrated leaf margins.

An alternative method is to represent the shape completely as a 1D curvature map which is then used for matching; this method has been suggested for generic shape matching [8], though has not been particularly popular. This is perhaps due to the higher computational demand compared with other methods which typically achieve similar results for generic shapes. An improvement over curvature maps are LAII [17]; these are largely analogous to curvature maps, though with the additional property of retaining locality of features over scale and are the representation used in this paper.

Leaf identification is also a well established problem in computer vision, again with a vast array of proposed techniques. Most methods use basic shape features including solidity, circularity, convexity and eccentricity [2, 18, 11, 25, 10, 12, 13]. Some also use more complex shape features such as Zernike moments [11], bending energy [2], histograms of curvature scale (HoCS) [15, 18], centroid radial maps [19] and Shen features [10]. [16] also includes features specifically targeted at the leaf margin to represent this information specific to leaf classification.

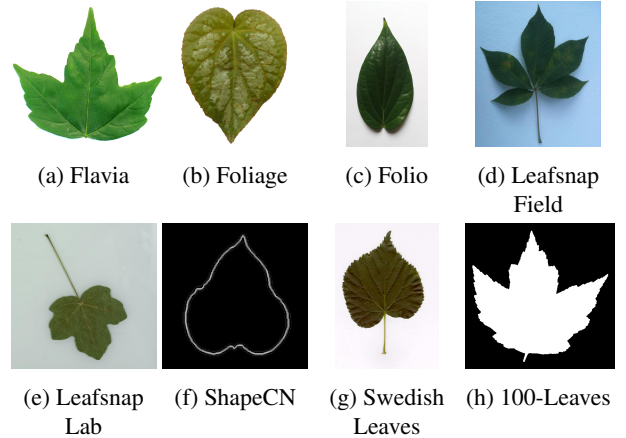
Colour features have been used, along with texture and vein features typically based on grey level co-occurrence matrix features (GLCM) [11, 12, 10, 13, 19]. Local binary variance patterns (LBVP) can also provide a basis for texture features [18].

Deep learning approaches have been attempted with the end-to-end training of large CNNs [3, 20, 7], though most methods follow a classical machine learning pipeline, most often using SVM or kNN classifiers, with some investigation into neural network classifiers [25, 13, 11].

1.4. Leaf Datasets

A number of publicly available leaf datasets are used to provide a good indication of the performance of the proposed methodology and its generalisability, these are summarised in Table 1. Example images from each dataset are visible in Fig. 1. Most datasets contain full colour images, though ShapeCN consists of black and white images in which the boundary of the leaf is marked with a single

Figure 1: Example images from leaf datasets.



pixel wide line and the 100-Leaves dataset contains black and white filled segmentations of leaf shapes.

Conditions in which the images are taken vary more significantly; some datasets contain colour images isolated against a flat white background, while others are taken in the field where leaves are placed on white paper in varying lighting conditions with shadows and blur often present, and some contain images of pressed leaves under lab conditions, typically on a backlit surface. The size, number of species and number of images per species also varies widely between datasets, including large imbalances between classes. The number of test images per species has mostly been chosen to constitute approximately 20% of the dataset as a whole, balanced equally between classes. In cases where some classes contain far fewer images than others a test split less than 20% is used to ensure all classes have a sufficient number of training examples.

Specific alterations have also been made for certain datasets. The original Leafsnap dataset includes 185 tree species, though field images are missing for *Ulmus Procera*, and *Quercus Falcata* contains insufficient lab images. These classes are therefore discarded entirely for the purposes of this study, leaving 183 tree species. *Prunus Virginiana* and *Prunus Sargentii* contained a number of incorrectly labelled images and *Maclura Pomifera* contained duplicates of all lab images, these erroneous images were removed. Four field images of exceptionally low quality (such that no leaf boundary could be extracted) were also discarded.

The creators of the base ShapeCN dataset [1] also provide two additional datasets, one of which contains 6 copies of each leaf image rotated by random angles between 0 and 360 degrees, totalling 3600 images. The other includes 4 copies of each leaf image scaled up in increments of 25%, totalling 2400 images; hereafter these are referred to as ShapeCN-R and ShapeCN-S respectively.

Table 1: Summary of publicly available leaf image datasets.

Dataset	Image Type	Condition	Total Images	Number of Species	Total per Species	Test per Species
Flavia [25]	Colour	Isolated	1907	33	50–77	10
Foliage [11]	Colour	Isolated	7200	60	120	20
Folio [19]	Colour	Field/Isolated	637	32	18–20	4
Leafsnap Field [15]	Colour	Field	7440	183	10–145	5
Leafsnap Lab [15]	Colour	Lab (Pressed)	22809	183	40–268	10
ShapeCN [1]	Contour	N/A	600	30	20	5
Swedish Leaves [23]	Colour	Lab (Pressed)	1125	15	75	15
100-Leaves [16]	Segmentation	N/A	1600	100	16	4

2. Implementation

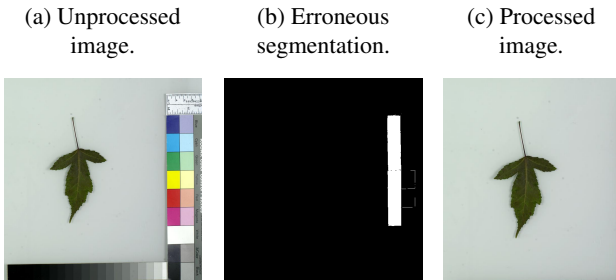
2.1. Preprocessing

Almost all datasets contain images that are ready to be used directly for extraction of LAII, but Leafsnap Lab images often include size and colour charts such as in Figure 2a. These present a significant disruption to the segmentation procedure, and for Leafsnap caused many erroneous segmentations like that of Figure 2b.

To combat this, the Leafsnap Lab images are first processed to remove the charts from the edges of the images. A threshold is applied to the saturation channel and greyscale images and the results summed together. Vertical and horizontal 10 pixel wide lines are then swept in from the right and bottom of the resulting image respectively, if the mean intensity of the image area defined by the line is below a threshold, and the previous mean value is above a certain threshold (i.e. the line has passed from the chart to the empty space to the left or above), then the current y or x position of the line is taken as the edge of the chart. The image is then cropped to these extremes, resulting in images like that shown in Figure 2c.

In a few cases this procedure failed and the charts were removed manually, a small number of images were also manually cropped to better centre the leaf within the frame.

Figure 2: Example image of *Acer Ginnala* from the Leafsnap Lab dataset.



2.2. Segmentation

The task of segmentation for the majority of datasets is trivial, some already contain segmentations or contours which can be used directly. Most others contain isolated leaves which can easily be segmented by a simple grey-level threshold. Lab and field images with variable backdrops pose a more significant challenge.

For those images the maximum of the mean values of the pixels along each edge of the image is used to determine the background saturation and grey-level which are then used as a basis for thresholding. A morphological closing operation is performed on the two resulting thresholds with a circular kernel of radius 5 pixels and the results summed to obtain a final segmentation for the image.

Once segmented, the stems are removed from the leaves as these drastically effect the LAII and vary randomly between leaves. This is achieved by applying a morphological top-hat operation to the segmentation with a square kernel (sized proportional to image resolution) and subtracting the result from the original segmentation. If the area of the segmentation would be reduced by more than 10% by applying the top hat operation (e.g. for thin pine needles) then this operation is not applied.

Once the initial segmentation is obtained, OpenCV’s [5] contour detection algorithm is used to find all contours in the image. For isolated and pre-segmented images there is typically only a single contour which can be used directly. For lab and field images there may be a number of other contours present caused by irrelevant objects in the images or lighting effects.

To select the most likely candidate contour, the contour with the largest area, that has a length greater than a fixed minimum and that is within a reasonable distance (proportional to image resolution) from the centre of the image is used. This procedure eliminates most errors due to lighting effects (which typically occur at the edge of images) and any small irrelevant objects in the image. If no suitable contour is found then a fallback method using canny edge detection [6] is used.

2.3. LAII Extraction

LAII are extracted using the method presented in [17], which is also used in [15] and [18]. A small circular mask is moved around the edge of the shape and a bitwise-and operation applied to obtain the intersection of the mask with the segmentation. The curvature at a given point is approximated as the proportion of the circle which is filled (i.e. the ratio of the area of the intersection to the area of the entire mask). A visualisation of one step in this process is shown in Figure 3.

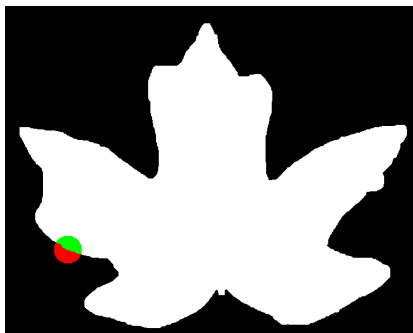
A fixed number of points are selected around the shape boundary, 256 is chosen for this application. LAII are extracted at multiple scales by varying the radius of the mask, the radius is defined as a percentage of the length of the contour to help retain scale invariance, this application makes use of 5 scales: 1%, 2.5%, 5%, 10% and 15%.

Examples of LAII for two leaf types can be seen in Figure 4, the first at the 1% scale and the second at 10%. Figure 4a shows a leaf with a serrated margin, but a relatively simple overall shape, while Figure 4b shows a leaf with a smooth margin, but more complex overall shape.

These differences are reflected in the LAII at both scales, with the 1% LAII for Figure 4a containing lots of high frequency activity, while its counterpart in 4b contains noticeably less. Meanwhile, the 10% LAII for 4a contains little low frequency activity and some low amplitude, high frequency activity, while for 4b contains noticeably more low frequency activity and almost no high frequency activity. Looking closely, the exact shape of each leaf can be seen to correspond directly to each LAII.

At low resolutions the LAIIs begin to be affected by pixel level artefacts and are prone to large amounts of noise. For the ShapeCN dataset which contains 256×256 pixel images, the 1% and 2.5% scales are discarded for this reason, improving accuracy by over 5%. This is not true for higher resolution images for which these smaller scales aid performance significantly.

Figure 3: Curvature map extraction method; circular mask shown against segmentation image with intersection in green and non-intersecting region of mask in red.



2.4. Feature Extraction

Once a valid contour has been obtained, a number of features are extracted. These fall into two broad categories; features based on the overall shape of the leaf and features based on the LAII. LAII are a 1D signals much like audio or ECG/EEG data, consequently many of the LAII features selected are inspired by feature extraction techniques typically used for these more common 1D signals.

2.4.1 Basic Shape Features

Four basic shape features are extracted and are surprisingly descriptive alone, achieving 75% accuracy on Flavia. Performance is much worse, though, for datasets with a larger number of species separated only by, for example, differences in margin characteristics (e.g. 48% accuracy on Leafsnap Lab).

Solidity

Solidity is the ratio of the contour area, a_c , to the area of the convex hull, a_h , for the contour.

$$\text{solidity} = \frac{a_c}{a_h}$$

Circularity

Circularity is the ratio of the area of the contour, a_c to the area of a circle with equal perimeter to the length of the contour, l_c .

$$\text{circularity} = \frac{4\pi a_c}{l_c^2}$$

Rectangularity

Rectangularity is the ratio of the area of the contour, a_c , to the area of the minimum-area rectangle containing the contour, of width w and height h .

$$\text{rectangularity} = \frac{a_c}{wh}$$

Compactness

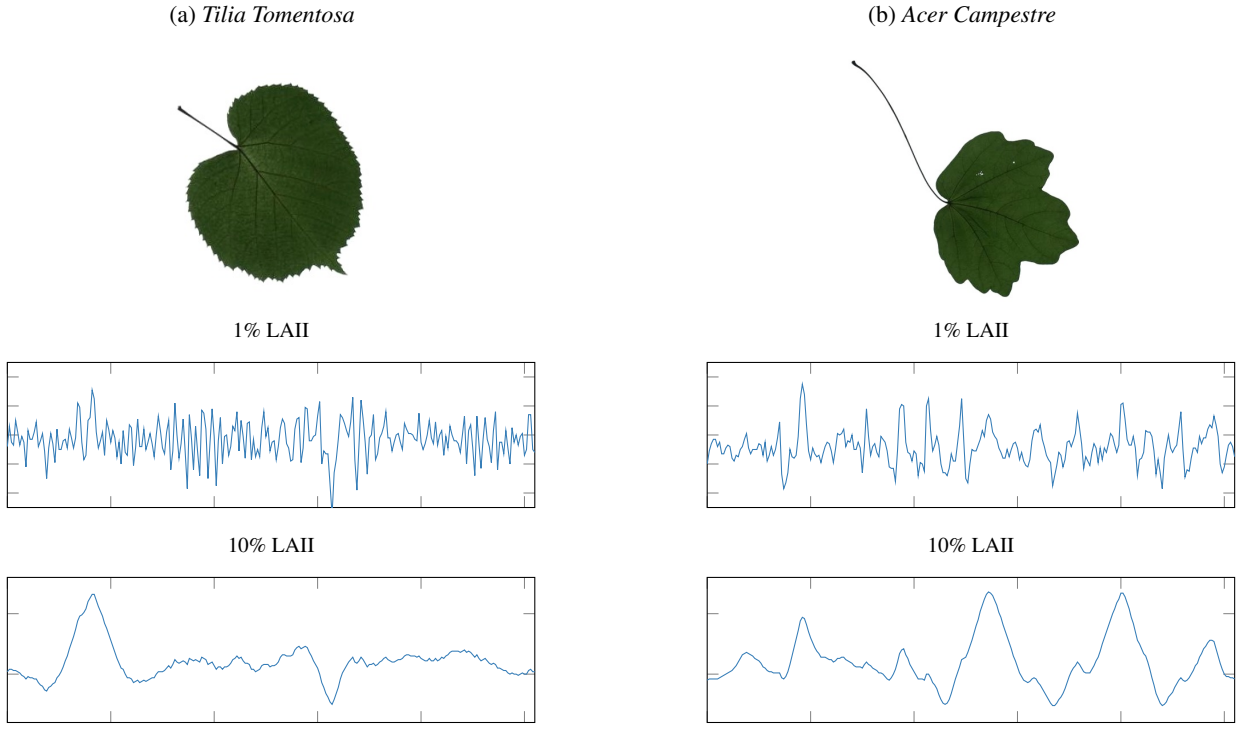
Compactness is the ratio of the length of the contour, l_c , to the area of the contour, a_c .

$$\text{compactness} = \frac{l_c}{a_c}$$

Exclusions

Some additional features were investigated, but found to have generally detrimental effects on performance. Eccentricity, the ratio of the height of the minimum-area rectangle to its width, and convexity, the ratio of the length of the perimeter of the convex hull to the length of the contour, were both excluded.

Figure 4: Leaf image and extracted LAII at small and large scales for two example leaves from the Leafsnap Lab dataset.



2.4.2 LAII Features

The majority of features are extracted from the LAIIs at the 5 different scales as described above. These features are predominantly statistical, as well focussing on the frequency spectra of the LAII, as is common for audio and ECG/EEG data.

Basic Statistical

The mean and standard deviation of each LAII, first and second differences, and absolute first and second differences are used. The area under the curve is also included to give some indication of the peaks present in the LAII.

Bending Energy

The bending energy, B , denotes the energy stored in a shape and has been used for leaf identification before [2]. It is defined as the mean value of the squared entries in a sequence, k_i , of length K .

$$B = \frac{1}{K} \sum_{i=1}^K k_i^2$$

Signal Entropy

Signal entropy is also used as a feature, calculated from a 128-bin histogram of each LAII.

Frequency (FFT)

The 256-bin real-valued FFT of the LAII, from this the spectral centroid, a feature typically used for audio, is calculated as shown. f_i being the frequency for a given FFT bin, and k_i the corresponding value for that bin.

$$\text{centroid} = \frac{\sum_{i=1}^K f_i k_i}{\sum_{i=1}^K k_i}$$

The centroid and full, normalised FFT for each LAII are included in the feature set.

Exclusions

A number of additional LAII-based features were investigated and excluded as they were found to be detrimental to performance. Zero crossing rate of the mean subtracted LAII was intended to give an indication of the number of significant shape features, but appeared to be too noisy, particularly for smaller scale LAII, and did not discriminate well between species.

Local binary patterns were also considered given their usage for EEG signals [14], but again didn't provide any significant benefit. Autocorrelation was explored as a method to highlight significant shape features and remove noise, but also had no positive effect on performance. This was likely due to reduction of signal elements corresponding to the leaf margin.

2.5. Classification

The full feature set contains 719 individual features; PCA is used to reduce the dimensionality to 128. This vastly improves training times with almost no effect on classification performance.

Classification is performed using an SVM with an RBF kernel ($C = 1000$, $\gamma = 7$) and balanced class weights. ScikitLearn's [21] SVM one-vs-one multi-class classification is used; a number of other classifiers were investigated, though none equalled the performance of the SVM.

Hyperparameters are selected to give good overall performance on all datasets; better results could be achieved by tuning hyperparameters for each dataset individually.

3. Results

3.1. Leaf Images

The presented methodology is first evaluated on the standard leaf datasets described in Table 1. The classification performance for each dataset is given in Table 2.

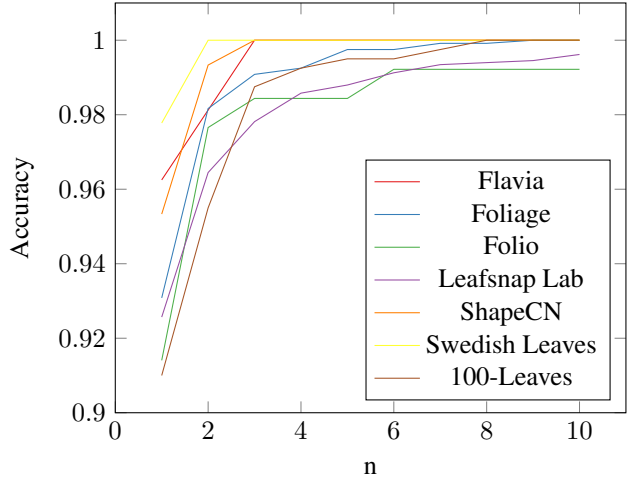
All datasets apart from Leafsnap Field achieve over 90% recall and precision for the first prediction, with the highest being Swedish Leaves at 97.8% recall. Leafsnap Field has significantly worse performance, with just 64.9% of first predictions correct. This is likely due to the poor quality of the input images, with large disruption caused by blur and shadows resulting in inaccurate segmentations.

The higher quality field images of Folio have caused much less of an issue, demonstrating that this method is robust to some level of shadow, but deals poorly with extreme lighting conditions and blur. An improved segmentation technique may aid performance in this case, though it is certainly clear that a high quality segmentation is required for effective LAII extraction.

Results for Flavia and Foliage, the two most commonly used datasets, are comparable with existing methodologies which make use of colour and texture features as well as shape. Reported accuracies range between 85% and 97% for Flavia and between 90% and 93% for Foliage. The presented method also performs comparably to existing approaches for other datasets, with the exception of Leafsnap Field, where a significantly higher first prediction accuracy of ~73% is reported, though with a somewhat unclear testing methodology.

Figure 5 demonstrates how, while first prediction accuracy is often in the low nineties, it rapidly improves (4% on average between top-1 and top-2 accuracy) and all datasets achieve over 98% accuracy for the top-4 predictions. So, while a few very similar leaf species might be confused, the presented methodology effectively separates these closely related species from the many other species present in the dataset. Only two of the seven included datasets fail to achieve 100% accuracy after 9 predictions.

Figure 5: Top-n accuracy scores for standard datasets (excluding Leafsnap Field).



3.2. Scale and Rotation Invariance

In order to evaluate the invariance to scale and rotation of the proposed methodology, an SVM is trained on the entire base ShapeCN dataset (600 images), this is then used to make prediction for the entire ShapeCN-R (3600 images) and ShapeCN-S (2400 images). As the ShapeCN-R and ShapeCN-S datasets only contain processed versions of the images contained in ShapeCN, the imbalance of training to testing samples is somewhat reasonable.

The results of this evaluation are shown in Table 3, along with the classification results for the standard dataset as above for comparison. The model performs comparably or better for both the rotated (98% recall) and scaled (97% recall) datasets indicating that this method is indeed invariant to scale and rotation of shapes within the images being classified.

The images in the ShapeCN-S dataset are provided at 512×512 pixels, while ShapeCN and ShapeCN-R both contain 256×256 pixel images. Using the larger ShapeCN-S directly resulted in significantly reduced performance (~10–15%), rescaling the images to 256×256 pixels eliminates this performance loss, demonstrating that while the method is largely invariant to the scale of the leaf within the image, the resolution of the input image does impact performance.

3.3. Generalisability

In addition to leaf images, [1] provides a set of 11000 black and white segmentation images of fish. 1100 classes of fish are included with 10 images per fish, these 10 are scaled (in increments of 25%) and randomly rotated versions of a single image. As such, a test set of 5 images per class is selected, leaving a training set containing 5 images per class.

Table 2: Classification performance for standard datasets.

	Flavia	Foliage	Folio	Leafsnap Field	Leafsnap Lab	ShapeCN	Swedish Leaves	100-Leaves
Recall	0.966	0.930	0.922	0.649	0.924	0.967	0.978	0.910
Precision	0.970	0.932	0.938	0.696	0.928	0.972	0.979	0.924
F1-Score	0.965	0.929	0.918	0.636	0.922	0.965	0.978	0.908

Table 3: Performance for ShapeCN-R and ShapeCN-S.

	Standard	Rotated	Scaled
Recall	0.967	0.980	0.967
Precision	0.972	0.980	0.970
F1-Score	0.965	0.980	0.968

Table 4: General shape classification performance.

	ShapeCN Fish	MPEG-7
Recall	0.989	0.911
Precision	0.991	0.936
F1-Score	0.989	0.910

The MPEG-7 Core Experiment dataset [22] is another public dataset for shape classification which includes 1400 black and white segmentation images split between 70 classes, each class contains 20 images. The images in the MPEG-7 dataset are significantly more diverse than the ShapeCN fish dataset; for this evaluation a test set containing 4 images per class is randomly selected.

The same extraction and classification procedure as for the leaf datasets is used to classify images from these generic shape datasets, results are given in Table 4. The high recall rates (99% and 91%) on these generic shape datasets indicate that the proposed LAII-based methodology provides a strong candidate for generic shape recognition tasks, providing accurate segmentation is possible.

4. Discussion

4.1. Future Work

The poor performance for the Leafsnap Field dataset is clearly an area of focus for improvement. Better segmentation, particularly dealing with shadows around the leaf edge, would most likely make the greatest difference. Blur is a potentially unsolvable problem, as leaf margin information may be irretrievably lost.

The stem removal procedure may also be sub-optimal; the top-hat operation removes thin areas around the edge of the leaf (e.g. at the end of pointed leaf leaves) which may

reduce performance through loss of true shape. Reliably determining which area of a leaf is the stem for such a large variety of shapes is a difficult challenge, simply taking the ratio of the principle moments of the region is insufficient to discriminate stems reliably as suggested in [15].

A similar challenge was presented by compound leaves, those consisting of multiple leaflets connected by a thin stem. Stem removal often isolates each leaflet or creates multiple groups of leaflets, only one of which is then taken forward as the final contour. Not removing stems retains the connection of the leaflets, but often includes a long additional stem section which disrupts extracted LAII and hampers classification. Some method to remove only the undesirable section of the stem and retain the sections connecting leaflets would likely provide the best results. [18] and [15] present potential methods to do just this, but are very inefficient.

A brief investigation into this and the above issue was unable to achieve suitable results so the simple top-hat operation was retained, future work would certainly benefit from further investigation.

The implementation of LAII extraction used in this paper can certainly be further optimised, [15] proposes a method to reduce the required calculations at each step which might be utilised. Using fewer scales would also improve extraction speed, though was found to reduce performance significantly. An improved LAII extraction method, perhaps incorporating smoothing to eliminate pixel-level effects, may help to enable the use of fewer scales.

4.2. Conclusion

This paper has presented a novel feature set for shape only leaf identification based on basic shape and LAII signal features. This methodology was evaluated on a number of publicly available leaf datasets with comparable results to existing methods which use colour and texture features in addition to shape. Over 90% accuracy was achieved on all datasets excluding Leafsnap Field, with top-four accuracy over 98%. Rotation and scale invariance of the feature extraction process was demonstrated, along with evaluation of the generalisability of the approach; achieving 91% accuracy on the MPEG-7 Core Experiment dataset of generic shapes.

Acknowledgements

Thanks to Dr. David Sinclair for his insights and advice throughout this investigation.

References

- [1] A. R. Backes, D. Casanova, and O. M. Bruno. A complex network-based approach for boundary shape analysis. *Pattern Recognition*, 42(1):54–67, 2009.
- [2] A. Backhaus, A. Kuwabara, M. Bauch, N. Monk, G. Sanguinetti, and A. Fleming. LEAFPROCESSOR: a new leaf phenotyping tool using contour bending energy and shape cluster analysis. *New phytologist*, 187(1):251–261, 2010.
- [3] P. Barré, B. Stöver, K. Müller, and V. Steinhage. LeafNet: A computer vision system for automatic plant species identification. *Eco-logical Informatics*, 40, 05 2017.
- [4] S. Belongie, J. Malik, and J. Puzicha. Shape matching and object recognition using shape contexts. *IEEE transactions on pattern analysis and machine intelligence*, 24(4):509–522, 2002.
- [5] G. Bradski. The OpenCV Library. *Dr. Dobb's Journal of Software Tools*, 2000.
- [6] J. Canny. A computational approach to edge detection. *IEEE Transactions on Pattern Analysis and Machine Intelligence*, PAMI-8(6):679–698, Nov 1986.
- [7] İ. Çuğu, E. Şener, Ç. Erciyies, B. Balci, E. Akin, I. Önal, and A. O. Akyüz. Treelogic: A novel tree classifier utilizing deep and hand-crafted representations. *arXiv preprint arXiv:1701.08291*, 2017.
- [8] G. Dudek and J. K. Tsotsos. Shape representation and recognition from curvature. In *Computer Vision and Pattern Recognition, 1991. Proceedings CVPR'91., IEEE Computer Society Conference on*, pages 35–41. IEEE, 1991.
- [9] C. Hewitt. TreeId source code. <https://github.com/friggog/tree-id>, Feb 2018.
- [10] A. Kadir. A model of plant identification system using glcm, lacunarity and shen features. *arXiv preprint arXiv:1410.0969*, 2014.
- [11] A. Kadir, L. Nugroho, A. SUSANTO, and P. Santosa. Experiments of zernike moments for leaf identification. *Journal of Theoretical and Applied Information Technology*, 41:82–93, 07 2012.
- [12] A. Kadir, L. E. Nugroho, A. Susanto, and P. I. Santosa. Leaf classification using shape, color, and texture features. *arXiv preprint arXiv:1401.4447*, 2013.
- [13] A. Kadir, L. E. Nugroho, A. Susanto, and P. I. Santosa. Neural network application on foliage plant identification. *arXiv preprint arXiv:1311.5829*, 2013.
- [14] Y. Kaya, M. Uyar, R. Tekin, and S. Yıldırım. 1d-local binary pattern based feature extraction for classification of epileptic eeg signals. *Applied Mathematics and Computation*, 243:209–219, 2014.
- [15] N. Kumar, P. N. Belhumeur, A. Biswas, D. W. Jacobs, W. J. Kress, I. Lopez, and J. V. B. Soares. Leafsnap: A computer vision system for automatic plant species identification. In *The 12th European Conference on Computer Vision (ECCV)*, October 2012.
- [16] C. Mallah, J. Cope, and J. Orwell. Plant leaf classification using probabilistic integration of shape, texture and margin features. *Signal Processing, Pattern Recognition and Applications*, 5(1), 2013.
- [17] S. Manay, D. Cremers, B.-W. Hong, A. J. Yezzi, and S. Soatto. Integral invariants for shape matching. *IEEE Transactions on pattern analysis and machine intelligence*, 28(10):1602–1618, 2006.
- [18] E. Mata-Montero and J. Carranza-Rojas. A texture and curvature bimodal leaf recognition model for identification of costa rican plant species. In *Computing Conference (CLEI), 2015 Latin American*, pages 1–12. IEEE, 2015.
- [19] T. Munisami, M. Ramsurn, S. Krishnah, and S. Pudaruth. Plant leaf recognition using shape features and colour histogram with k-nearest neighbour classifiers. *Procedia Computer Science*, 58:740–747, 2015.
- [20] P. Pawara, E. Okafor, O. Surinta, L. Schomaker, and M. Wiering. Comparing local descriptors and bags of visual words to deep convolutional neural networks for plant recognition. In *ICPRAM*, pages 479–486, 2017.
- [21] F. Pedregosa, G. Varoquaux, A. Gramfort, V. Michel, B. Thirion, O. Grisel, M. Blondel, P. Prettenhofer, R. Weiss, V. Dubourg, J. Vanderplas, A. Passos, D. Cournapeau, M. Brucher, M. Perrot, and E. Duchesnay. Scikit-learn: Machine learning in Python. *Journal of Machine Learning Research*, 12:2825–2830, 2011.
- [22] R. Ralph. Mpeg-7 core experiment ce-shape-1. 1999.
- [23] O. Söderkvist. Computer vision classification of leaves from swedish trees. Master's thesis, Linköping University, sep 2001.
- [24] A. Thayananthan, B. Stenger, P. H. Torr, and R. Cipolla. Shape context and chamfer matching in cluttered scenes. In *Computer Vision and Pattern Recognition, 2003. Proceedings. 2003 IEEE Computer Society Conference on*, volume 1, pages I–I. IEEE, 2003.
- [25] S. G. Wu, F. S. Bao, E. Y. Xu, Y. X. Wang, Y. F. Chang, and Q. L. Xiang. A leaf recognition algorithm for plant classification using probabilistic neural network. In *2007 IEEE International Symposium on Signal Processing and Information Technology*, pages 11–16, Dec 2007.